Energy Conversion and Management 78 (2014) 151–164

Contents lists available at ScienceDirect

Energy Conversion and Management

journal homepage: www.elsevier.com/locate/enconman

Economic-environmental energy and reserve scheduling of smart distribution systems: A multiobjective mathematical programming approach

Alireza Zakariazadeh [a], Shahram Jadid [a], Pierluigi Siano [b,*]

[a] Electrical Engineering Department, Iran University of Science and Technology (IUST), Iran
[b] Department of Industrial Engineering, University of Salerno, Fisciano, Italy

ARTICLE INFO

Article history:
Received 21 June 2013
Accepted 19 October 2013
Available online 18 November 2013

Keywords:
Distribution system
Emissions
Multi-objective optimization
Demand response
Wind power

ABSTRACT

In this paper a stochastic multi-objective economical/environmental operational scheduling method is proposed to schedule energy and reserve in a smart distribution system with high penetration of wind generation. The proposed multi-objective framework, based on augmented ε-constraint method, is used to minimize the total operational costs and emissions and to generate Pareto-optimal solutions for the energy and reserve scheduling problem. Moreover, fuzzy decision making process is employed to extract one of the Pareto-optimal solutions as the best compromise non-dominated solution. The wind power and demand forecast errors are considered in this approach and the reserve can be furnished by the main grid as well as distributed generators and responsive loads. The consumers participate in both energy and reserve markets using various demand response programs. In order to facilitate small and medium loads participation in demand response programs, a Demand Response Provider (DRP) aggregates offers for load reduction. In order to solve the proposed optimization model, the Benders decomposition technique is used to convert the large scale mixed integer non-linear problem into mixed-integer linear programming and non-linear programming problems. The effectiveness of the proposed scheduling approach is verified on a 41-bus distribution test system over a 24-h period.

1. Introduction

Air pollution and global warming have been recognized for years the main critical environmental issues in many countries. Accordingly, there has been an international movement in the promotion of renewable technologies for electricity generation and the development of national emissions limits [1]. A number of directives for controlling emissions are currently in place, that have particular impact on the electricity industry, such as the Kyoto Protocol [2], the Large Combustion Plant Directive [3], and the National Emissions Ceilings Directive [4]. Moreover, any imposed constraint on system operation results in an increase in operation costs and may have a detrimental effect on emissions [5]. With proper scheduling of electricity resources, such as low-carbon power plant technologies, renewable generation units and Demand Response (DR), the air pollutant emissions can be, however, reduced. The proper scheduling of electricity resources can be addressed by implementing the so called “smart grid” approach.

Demand response (DR) is one of the key approaches that can fully be enabled by smart grids. DR is a set of actions taken to reduce consumer electricity consumption when contingencies, such as unit outage or unpredictable change in demand or renewable generation, occur that threaten supply demand balance. Moreover, if market conditions that raise electric supply costs occur, DR is one of the best solutions. In other words, DR programs and tariffs may be designed to improve the reliability of the electric grid or to lower the use of electricity during peak hours, thus reducing the total system operation costs.

The implementation of real-time information systems, Advanced Metering Infrastructure (AMI), improved communication capabilities [6], intelligent sensors, and improved infrastructure for control systems will, in fact, transform the conventional distribution system into a Smart Grid [7]. It will bring flexibility in distribution system operations via online control of Distributed Energy Resources (DERs) and will allow demand side management programs actuation [8]. An energy management system (EMS) aiming at optimizing the smart grid’s operation has been proposed in [9]. The EMS behaves as a sort of aggregator of distributed energy resources allowing the SG participating in the open market. By integrating demand side management (DSM) and active management schemes (AMS), it permits an enhanced exploitation of

* Corresponding author. Tel./fax: +39 089964294.
E-mail addresses: zakaria@iust.ac.ir (A. Zakariazadeh), jadid@iust.ac.ir (S. Jadid), psiano@unisa.it (P. Siano).

0196-8904/$ - see front matter © 2013 Elsevier Ltd. All rights reserved.
http://dx.doi.org/10.1016/j.enconman.2013.10.051

renewable energy sources and a reduction of the customers' energy consumption costs with both economic and environmental benefits. In [10], a methodology for optimal reconfiguration of distribution networks integrated with an Optimal Power Flow (OPF) is presented. The Benders decomposition algorithm is applied for solving the problem. However, renewable generation and demand response programs are not considered.

On the other end, environmental concerns that arise due to the operation of fossil fuel fired electric generators, change the classical economic electricity operational planning problem into a multi-objective emission/economic operational planning problem [11–13]. A multi-objective emission/economic dispatch for transmission system based on AC load flow has been presented in [11]. In [12], a generation dispatch model with large scale wind systems is proposed in which environmental and fuel costs are modeled by using a multi-objective method. A multi-objective optimal power flow is used in [13] to simulate how the parties' incentives affect the choice of Distributed Generators (DGs) capacity within the limits of the existing network. The authors explored the costs, benefits and tradeoffs associated with DGs in terms of connection, losses and, in a simple fashion, network deferral.

In [14], a method for energy resource scheduling in smart distribution system has been presented in which day, hour and 5 min ahead scheduling were considered. The short-term scheduling has been used to re-schedule the previously obtained program taking advantage of the better accuracy of short-term wind forecasting in order to obtain more efficient resource scheduling solutions. In [15], an agent-based model has been used to validate a smart grid environment. Moreover, the paper presented a method based on demand able to mitigate the impact of wind power variability, primarily through thermostatically controlled loads. The result showed that a smarter grid has the potential to balance fluctuations and intermittencies occuring when multiple and intermittent suppliers are integrated into the distribution system. A methodology for day-ahead energy resource scheduling in a smart distribution system has been presented in [16]. DG units and electric vehicles as well as the distribution network constraints have been taken into account in the model. Also, the paper focused on the reduction of the execution time allowed by the proposed model by using a modified particle swarm optimization.

In this paper a multi-objective approach for energy and reserve scheduling of distribution systems is presented in which various types of demand response programs are taken into account. The innovative contributions of the proposed method are highlighted as follows:

- Include and aggregate wind generation and load demand uncertainties in distribution systems operational planning model.
- Evaluate load demand participations in both energy and reserve scheduling.
- Include the emission reduction target in distribution systems operation.

The rest of the paper is organized as follows: Section 2 describes different types of demand response programs. Wind generation and electricity demand uncertainties are modeled in Section 3. In Section 4, the stochastic scheduling of energy and reserve is formulated. Some simulation results are described in Section 5, and finally concluding remarks are presented in Section 6.

2. Demand response programs and providers

In this section the different types of demand response models used in this paper are described. The way DR agents participate in these DR programs is also presented.

2.1. Demand response programs

The demand response programs implemented in the proposed method are categorized in demand energy reduction and demand reserve as follows [17].

2.1.1. Demand bidding/buyback programs

Demand bidding/buyback programs encourage heavy consumers (like industrial and commercial loads) to offer load reductions at a price at which they are willing to be curtailed.

2.1.2. Ancillary Services Market Programs

In this type of programs, customers can bid load curtailment as reserve capacity for the system. If their bids are accepted, they are paid at the reserve price for their involvement and for remaining in standby. If their load curtailments are needed, they are called by the Independent System Operator (ISO) or Distribution System Operator (DSO), and can be also paid at their accepted offer price for load reduction.

2.2. Demand Response Service Provider (DRSP)

Service Providers (SPs) are defined as the organizations providing services to electrical customers and to utilities. An electric utility may be a SP, but that is not essentially the case. In some states, such as Texas, the electricity market has been restructured so that a SP may be a company completely distinct from the electric utility and customers can choice among competing SPs. Several third-party service providers offer demand response aggregation, energy management services, and other similar offers [18].

Actors in the service provider domain carry out services to support the business processes of electric network producers, distributors, and customers. These business processes range from conventional utility services, such as billing and customer account management, to improved customer services, such as management of energy use and home energy generation.

Demand Response Providers (DRPs) are also some types of SPs that provide demand response services to electrical customers and to utilities. DRPs aggregate small electricity customer's response; they register smaller customers, aggregate their offers, and submit the aggregated offers on behalf of them in the wholesale market. DRPs are to be paid for their services if they improve the operation of the electric grid. An Energy Services Interface (ESI) serves as the information management gateway through which the customer domain interacts with DRPs. The DRP acts as a medium between DSO and small customers and enables the participation of small customers in the DR programs.

In this paper, some DRPs are defined in order to aggregate offers for load reduction made by their determined consumers. Fig. 1 depicts a typical price–quantity offer package containing four pairs where o_ψ is price offer in step ψ. For each hour, a DRP submits its price–quantity offer as a package. Each step in the typical price–quantity offer package submitted by a customer that is willing to reduce its consumption is shown in Fig. 1. At each hour, L_{Max} is the sum of all loads reduction and L_{Min} is the minimum load reduction that a customer can carry out. For example, let assume that in an energy scheduling procedure, L_3 kW of load reduction are accepted from a DRP. The DRP is paid at o_1 for L_1, o_2 for $L_2 - L_1$, and o_3 for $L_3 - L_2$. The equations for the ith DRP are the following ones from (1)–(4).

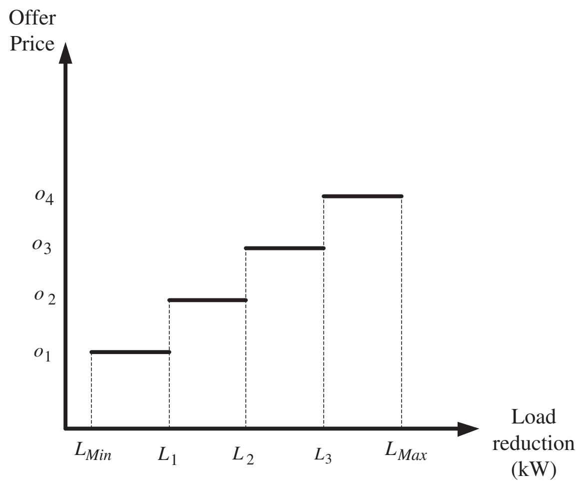

Fig. 1. The steps price–quantity offered package of DRP.

$$L^i_{Min} \leqslant l^i_1 \leqslant L^i_1 \tag{1}$$

$$0 \leqslant l^i_\psi \leqslant \left(L^i_{\psi+1} - L^i_\psi\right) \quad \forall \psi = 2, 3, \ldots \tag{2}$$

$$DP^E(i,t) = \sum_{\psi=1} l^i_\psi \tag{3}$$

$$DC^E(i,t) = \sum_{\psi=1} o^i_\psi \cdot l^i_\psi \tag{4}$$

where l^i_ψ is the accepted load reduction of DRP i at step ψ of the price–quantity offer package; $DP^E(i,t)$ and $DC^E(i,t)$ are, respectively, the total accepted load reduction quantity and payment for the ith DRP in period t.

At each hour, the sum of scheduled energy reduction and reserve provided by each DRP should not be greater than its maximum load reduction offer $\left(L^i_{Max}\right)$. This means that the uncommitted load reduction capacity of each DRP's offer package during energy scheduling can be also scheduled for reserve requirement. The reserve prepared by DRPs is calculated as follows:

$$DP^E(i,t) + DP^R(i,t) \leqslant L^i_{Max} \tag{5}$$

$$DC^R(i,t) = DP^R(i,t) \times q^{R,p}(i,t) \tag{6}$$

where $DP^R(i,t)$ and $q^{R,p}(i,t)$ are the scheduled reserved provided by DRP i and the reserve price for being in standby in period t, respectively; L^i_{Max} is the maximum quantity of load reduction offered by DRP i, and $DC^R(i,t)$ is the reserve cost that is paid to DRP.

On the other hand, large consumers, corresponding to industrial and commercial customers, can directly participate in DR programs. These consumers offer their quantity–price pair offers for load reduction or in order to provide reserve to the system operator. The equations of individual loads (ILs), participating in both energy reduction and reserve supply programs, are given as follows:

$$IL^E(b,t) + IL^R(b,t) \leqslant IL^{max}_b(b,t) \tag{7}$$

$$IC^E(b,t) = IL^E(b,t) \times q^{E,l}(b,t) \tag{8}$$

$$IC^R(b,t) = IL^R(b,t) \times q^{R,l}(b,t) \tag{9}$$

where $IL^E(b,t)$ and $IL^R(b,t)$ are, respectively, the scheduled load reduction and reserve prepared by consumer b in period t; $IL^{max}_b(b,t)$ is the maximum load reduction offered by consumer b in period t; $q^{E,l}(b,t)$ and $q^{R,l}(b,t)$ are the price offers of consumer b for energy reduction and for being in standby for reserve in period t, respectively. The cost of load reduction and committing reserve, that are paid to individual loads participating in DR programs, are $IC^E(b,t)$ and $IC^R(b,t)$, respectively.

3. Wind generation and demand uncertainty modeling

In this section, the wind generation and demand modeling considered in the scheduling approach are explained.

3.1. Wind generation modeling

The Rayleigh probability density function (PDF) is regularly used as a proper expression model of wind speed behavior [19]. Rayleigh PDF is a special case of Weibull PDF in which the shape index is equal to 2.

$$f(v) = \left(\frac{2v}{c^2}\right) \exp\left[-\left(\frac{v}{c}\right)^2\right] \tag{10}$$

where (v), c and v are Rayleigh PDF, scale index and wind speed, respectively. If the mean value of the wind speed (v_m) for a site is known, then the scaling index c can be calculated as in (11) and (12)

$$v_m = \int_0^\infty v f(v)\, dv = \int_0^\infty \left(\frac{2v^2}{c^2}\right) \exp\left[-\left(\frac{v}{c}\right)^2\right] dv = \frac{\sqrt{\pi}}{2} c \tag{11}$$

$$c \simeq 1.128\, v_m \tag{12}$$

In order to integrate the output power of the wind-based DG units as a multi-state variable in the distribution energy scheduling formulation, the continuous Rayleigh probability density function has been divided into intervals, in each of which the wind speed is within specific limits. The number of intervals is carefully selected for the Rayleigh distribution because a small number of intervals decreases the accuracy, whereas a large number increases the problem complexity. A 5-interval wind speed probability distribution function is illustrated in Fig. 2. The probability of each interval (P_w) is calculated using Eq. (13):

$$p_w = \int_{v_{w1}}^{v_{w2}} f(v)\, dv \tag{13}$$

where v_{w1} and v_{w2} are the speed limits of interval w. The output power of the wind turbine corresponding to each interval, is calculated by using the wind turbine power curve parameters as described by Eq. (14). In order to simplify the analysis, the average value of each interval (v_{aw}) is used to calculate the output power for each interval.

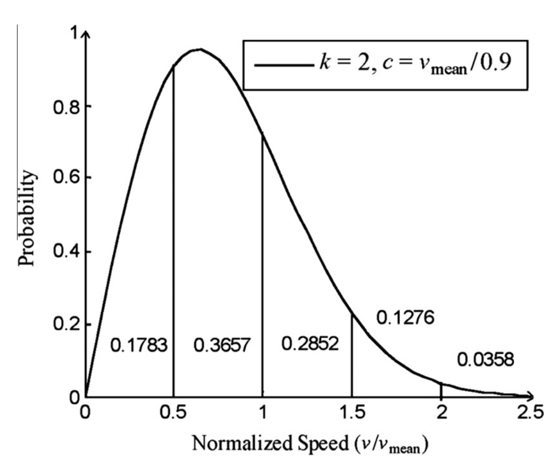

Fig. 2. An indicative wind speed distribution model.

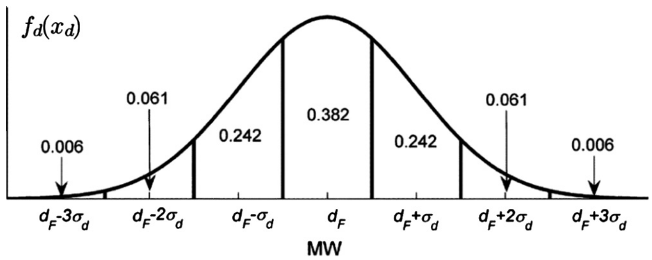

Fig. 3. Seven-interval approximation of the Gaussian distribution.

$$P_w(v) = \begin{cases} 0, & 0 \leqslant v_{aw} \leqslant v_{ci} \\ P_{rated} \times \frac{(v_{aw}-v_{ci})}{(v_r-v_{ci})}, & v_{ci} \leqslant v_{aw} \leqslant v_r \\ P_{rated}, & v_r \leqslant v_{aw} \leq v_{co} \\ 0, & v_{co} \leqslant v_{aw} \end{cases} \tag{14}$$

where v_{ci}, v_r and v_{co} are the cut-in speed, rated speed and cut-off speed of the wind turbine, respectively.

3.2. Load modeling

The power system operator should forecast the amount of demand at each of the following hours and days. As the anticipating process has some errors, the demand forecast will not be 100% accurate [20,21]. Thus, the uncertainty about future demand is modeled by a number of states. The demand forecast uncertainty is often modeled by a normal probability distribution function as illustrated in Fig. 3 [22–25]. For creating a limited number of demand states during each hour, it is generally sampled from the distribution curve shown in Fig. 3.

In the proposed model, the error associated to load demand is assumed to be normally distributed and the weights p_d are given by the area under the curve between the lower and upper limits of each interval j.

$$p_d = \frac{1}{\sigma_d\sqrt{2\pi}} \int_{l_j}^{u_j} e^{-(x-d_f)^2/2\sigma_d^2} d_x \tag{15}$$

where u_j and l_j are, respectively, the upper and lower limits of load demand in each interval; d_f and σ_d are the net forecast demand and the standard deviation for normal PDF, respectively.

3.3. Scenario combination

In order to combine different states of wind and demand fluctuations, the scenario tree model is used in the proposed method [26,27]. As seen from Fig. 4, each scenario consists of two different states of wind generation and demand forecasted values. Each scenario is assigned a weight π_s, that reflects the possibility of its occurrence. Scenarios considering possible wind power variation and demand fluctuation at each hour are taken into account.

4. The stochastic energy and reserve scheduling

In the proposed model, energy and reserve scheduling in the distribution network are managed by the DSO. The interactions between the DSO and other participants are shown in Fig. 5 [9,28,29].

In order to model the wind power generation and load demand uncertainties within the energy and reserve scheduling, a two-stage stochastic programming framework is implemented. In this procedure, the electrical energy required to supply demand loads should be scheduled while simultaneously considering the uncertainty associated to wind power and load demand. Hence, variables pertaining to the energy and reserve costs and payments that are

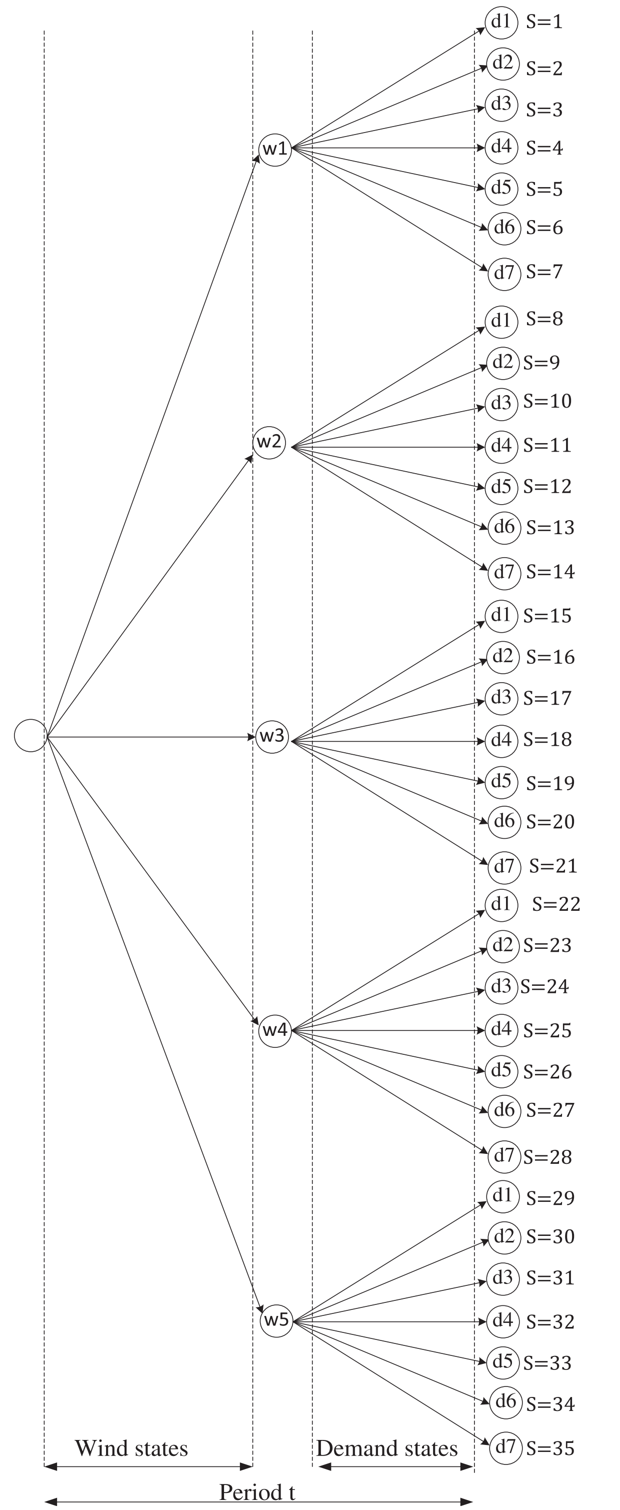

Fig. 4. Scenario tree for combination of wind generation and demand forecasted values.

made before the realization of any scenario should be considered in the first stage of this model. These variables for each time period include:

1. Scheduled input power from the main grid and scheduled power for DGs.
2. Scheduled load reduction for each individual load or DRP.

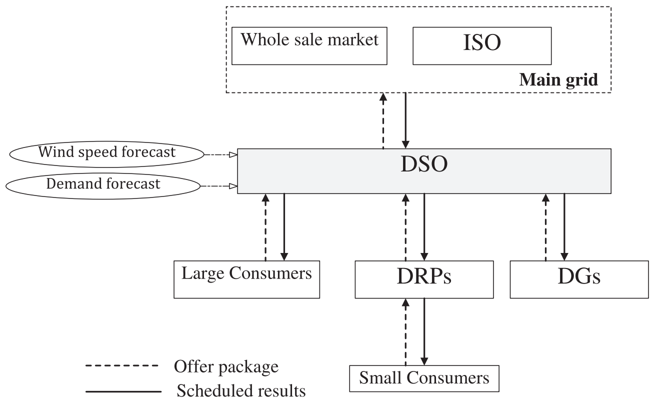

Fig. 5. Interactions between DSO and participants.

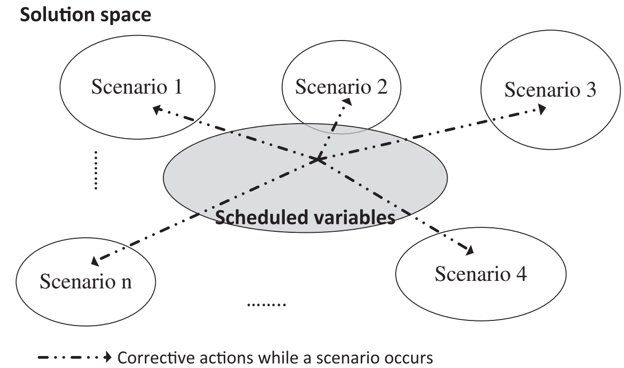

Fig. 6. The solution space of stochastic optimization.

3. Scheduled spinning reserve for the main grid and DGs.
4. Scheduled reserve for each individual load or DRP.

In the second stage of the model, variables pertaining to each particular scenario at each time period should be considered. These variables, which are related to the actual operation of the distribution system, include:

1. The dispatching (using) of scheduled spinning reserve committed by the main grid and DGs.
2. The dispatching (using) of scheduled reserve by each individual load or DRP.
3. The involuntarily load shedding by each consumer.
4. The wind power production.
5. The power flow variables, namely, voltage magnitudes and angles at each bus, power losses in every line, flow through each line and power injection at every bus.

The two-stage stochastic model presented in this paper for short term energy and reserve scheduling in a distribution system is formulated as a two-stage stochastic programming problem: the first stage denotes the day-ahead scheduling with its constraints, while the second stage denotes the distribution system operation and its constraints. In the proposed method, the scheduling variables pertaining to the first stage correspond to the market decisions, that also reflect the realizations of stochastic processes without being explicitly linked to one specific realization, but to all of them. The cost objective function to be minimized groups separately those terms representing the costs concerning the electricity market and those representing the costs incurred during the actual operation of the distribution system. In other words, in the distribution system operation procedure, after running the day-ahead scheduling program, the DSO should announce the scheduling results related to the required power and curtailed load demand to the ISO, DGs' owner and DR participants. The consequent related payments for all actors should be also determined.

In the first stage, the scheduling variables are, therefore, obtained as a result of the optimization procedure and used for determining the set points of DGs power, load demand reduction and main grid input power, as well as for payments calculation. The first stage variables (scheduled variable) do not belong to any scenario and are determined in order to announce the results and for payment calculation. Since the scheduling variables are not linked to one specific realization, but depend from all of them and due to wind generation and load demand uncertainties, the final dispatching results will be determined only during the real time operation. The scheduling variables, determined as a result of the first stage, will be, thus, different from the dispatching variables that are determined during the real time operation. Their difference will determine generation and consumption variations, as well as costs and payments changes, depending on what scenario will occur in real time.

The probability of each scenario will determine its importance and effect on the scheduled result. In Fig. 6, a simple solution space for a stochastic optimization problem is shown. Each scenario has an optimal solution according to its allocated wind generation and demand parameters. The scheduled variables should be determined in such a way that the cost of corrective actions for changing the scheduled parameters is minimized. The corrective actions comprise additional absorbed power from the main grid, additional load demand reduction or increment of power generation from DG units.

Scheduled variables represent the outputs of this model which determines the generation and consumption program of the distribution system through the next 24 h. It is worth noting that scheduled variables determine contracting amounts of electricity and reserve for that the DSO should pay to the electricity market operator and DRPs. The difference between active power variables of DGs and main grid as well as load demand reduction in the first and second stage are taken into account as reserve (corrective actions). In other words, a scenario variable determines the corrective actions that the operator should perform if that scenario happens in order to operate the system in a secure and economic mode. In each scenario, there is a tradeoff between the amount of reserve requirement and the expected energy not served.

The involuntarily load shedding is used in this model to prevent committing more reserve in some scenarios with low probability of occurrence and refers to unplanned load shedding in which the operator should pay damage cost for power interruptions. The need to cover all power curtailment due to wind generation and demand forecast errors by providing reserve, irrespective of their likelihood of occurrence, will decrease the overall social welfare and, particularly, may sharply increase the incremental costs of reserve and energy [30]. The Value of Lost Load (VOLL) is defined as the value that an average consumer loses from an unsupplied kWh of energy. The value of these reductions can be expressed as a customer damage function. While an involuntarily load shedding for a consumer occurs, the damage cost is paid at VOLL to this consumer. In the proposed two-stage stochastic model, the Energy Not Served (ENS) term in the second stage could affect the result of the first stage. In other words, the involuntary load shedding is required when the power shortage due to wind curtailment occurs in a scenario. If reserve is allocated in order to cover wind power curtailment, the involuntary load shedding is not required. So, the optimization method carries out a trade-off between ENS and reserve costs in order to minimize the total costs.

Let's assume, for example, that a diesel generator is scheduled to generate 800 kW power in a specific hour (first stage). In other hand, if a scenario where 200 kW of wind curtailment occurs, it is needed to compensate this power shortage by an energy resource like DGs, main grid power plants or demand response. Let's suppose in this period the diesel generator has the lowest energy cost, the scenario variable for the diesel generator is set at 1000 kW. It means that when this scenario occurs in real time, the diesel generator (that has been scheduled at 800 kW power output) should increase its power up to 1000 kW in order to cover the wind energy curtailment. So, this additional active power of 200 kW is calculated as a reserve for the diesel generator.

4.1. Assumptions

In this model the following assumptions are considered [28,31].

- Wind generation is assumed to be a regulated activity and thus wind producers are not considered competitive agents in the market and, thus, are paid at a regulated tariff.
- The distribution system operator (DSO) is responsible for energy and reserve scheduling in a distribution system. DSO purchases its energy and reserve requirements from the wholesale electricity market.
- The wholesale hourly electricity price for energy and reserve, as well as average emission rate of the main grid's power plants through the next 24-h period are available.

4.2. Objective function and constraints

The proposed distribution energy and reserve scheduling method aims at minimizing two objective functions: cost (F^{cost}) and emission ($F^{Emission}$). The stochastic multi-objective optimization problem is formulated as follows:

$$Minimize\{F^{cost}, F^{Emission}\} \tag{16}$$

The total expected cost (F^{cost}) of the distribution network represents one of the objective functions that should be minimized [25,32]. The cost objective function has two parts: the first one (CC) is the sum of contracting energy and reserve costs that should be paid to the market operator and to consumers participating in DR programs, while the second part represents the total operational costs associated to the considered scenarios.

The first part of cost objective function, representing the payment costs of electricity and reserve during the total scheduling horizon is given as follows:

$$\begin{aligned} CC = & \sum_{t=1}^{T}\Big[P_{grid}(t)\times Ta_g^E(t) + R_{grid}(t)\times Ta_g^R(t) \\ & + \sum_{j=1}^{J} C_{DG}(j,t) + R_{DG}(j,t)\times C_{DGj}^R(t) + \sum_{b\in Nl} IC^E(b,t) + IC^R(b,t) \\ & + \sum_{i\in I} DC^E(i,t) + DC^R(i,t) + \sum_{w=1}^{W}\lambda_t^w \times P_w(t)\Big] \end{aligned} \tag{17}$$

where $P_{grid}(t)$ and $R_{grid}(t)$ are, respectively, the scheduled purchased energy and reserve from the main grid in period t. $Ta_g^E(t)$ and $Ta_g^R(t)$ are the hourly and reserve price of energy, respectively; J is the number of DGs and $C_{DG}(j,t)$ represents the hourly fuel cost of DG j in period t; $R_{DG}(j,t)$ and $C_{DGj}^R(t)$ are the spinning reserve provided by DG j and the price of reserve, respectively; $P_w(t)$ and λ_t^w are the active power of wind turbine w and the cost of wind energy in period t, respectively [33–35].

The second part of cost objective function takes into account the operational costs associated to each scenario ($SC(s)$) that includes the costs associated to the energy as well as deployment of reserve for the considered scenario and its probability of occurrence ($\pi(s)$).

The operational cost associated to each scenario is given as follows:

$$\begin{aligned} SC(s) = & \sum_{t=1}^{T}\Big[Ps_{grid}(s,t)\times Ta_g^E + \sum_{j=1}^{J} Cs_{DG}(j,t,s) + \sum_{b\in Nl} IC^s(b,t,s) \\ & + \sum_{i\in I} DC^s(i,t,s) + ENS(s,t)\times voll(t)\Big] \end{aligned} \tag{18}$$

where $Ps_{grid}(s,t)$ is the required purchased power from the main grid in period t and scenario s; $Cs_{DG}(j,t,s)$ represents the operational cost of DG j in period t and scenario s; $DC^s(i,t,s)$ and $IC^s(n,t,s)$ are, respectively, the costs associated to both groups of load reductions in period t and scenario s, respectively; $ENS(s,t)$ and $voll(t)$ are the Expected Energy Not Served (EENS) and the Value of Lost Load (VOLL), respectively.

The fuel cost of a generator can be generally expressed as a function of its real power output and can be modeled by a quadratic polynomial [36]. The operational cost of a DG unit (like a diesel generator) with a quadratic cost function $C_{DG}(j,t)$ is given by [9]:

$$C_{DG}(j,t) = a_j \times u(j,t) + b_j \times P_{DG}(j,t) + c_j \times P_{DG}^2(j,t) \tag{19}$$

where a_j, b_j and c_j represent the cost coefficients of DGs; $P_{DG}(j,t)$ and $u(j,t)$ are the active output power and the binary variable which shows the on/off state of DG j in period t, respectively.

Accordingly, the DG cost in each scenario ($Cs_{DG}(j,t,s)$) is calculated as follows:

$$Cs_{DG}(j,t,s) = a_j \times us(j,t,s) + b_j \times Ps_{DG}(j,t,s) + c_j \times Ps_{DG}^2(j,t,s) \tag{20}$$

where $Ps_{DG}(j,t,s)$ and $us(j,t,s)$ are the active power and the on/off state of the DG j in period t and scenario s, respectively. In order to implement a linear programming approach, the non linear cost function of DG is approximated by a linear function that, for practical purpose, is indistinguishable from the non-linear model [37].

The cost objective function of the stochastic energy and reserve scheduling represents the total expected cost (F^{cost}) calculated as follows:

$$F^{cost} = CC + \sum_{s=1}^{S}\pi(s)\times SC(s) \tag{21}$$

where $\pi(s)$ is the probability of scenario s .

Electrical loads are supplied by both DGs installed in the distribution network and conventional power plants connected to the main grid. The emissions of non-renewable DGs (Emi^{DG}) are calculated as follows:

$$Emi^{DG} = \sum_{t=1}^{T}\sum_{j=1}^{J} E_{CO_2}^{DG}(j)\times P^{DG}(j,t) \tag{22}$$

where $E_{CO_2}^{DG}(j)$ is the CO_2 emission rate of DG j .

The average emissions due to the power plants of the main grid (Emi^{grid}) are calculated as follows:

$$Emi^{grid} = \sum_{t=1}^{T} E_{CO_2}^{grid}(t)\times P_{grid}(t) \tag{23}$$

where $E_{CO_2}^{grid}(t)$ is the average CO_2 emission rate of the power plants in period t.

The objective function related to the total emissions during the planning period is calculated as follows:

$$F^{Emission} = Emi^{grid} + Emi^{DG} \tag{24}$$

The following constraints are considered in the optimization problem.

4.2.1. Load balance

$$P_{grid}(t)+\sum_{j=1}^{J}P_{DG}(j,t)+\sum_{w=1}^{W}P_{w}(t) = P_{L}(t)+Loss(t)-\sum_{i}DP^{E}(i,t)-\sum_{b}IL^{E}(b,t) \quad \forall t \tag{25}$$

where $P_w(t)$ and $P_L(t)$ are the active power of wind turbine w and the active demand in period t, respectively; $Loss(t)$ represents the total energy losses in period t .

The energy balance at each scenario should also be satisfied.

$$Ps_{grid}(s,t)+\sum_{j=1}^{J}Ps_{DG}(j,t,s)+\sum_{w=1}^{W}P_{w}(s,t) = P_{L}(s,t)+Loss(s,t)-\sum_{b}IL^{s}(b,t,s)-\sum_{i}DP^{s}(i,t,s) - ENS(s,t) \quad \forall t,s \tag{26}$$

where $P_w(s,t)$ and $P_L(s,t)$ are the wind active power and the active demand in scenario s, respectively. The required load reduction from DRPs and large loads at each scenario are defined as $DP^s(i,t,s)$ and $IL^s(b,t,s)$, respectively. $ENS(s,t)$ is the amount of involuntarily load shedding at each scenario which should be subtracted from load demand. This amount of load reductions pertaining to a specific scenario is defined as the load reserve requirement for the condition in which this scenario occurs.

4.2.2. Demand response participants' constraints

The scheduled reserves prepared by DRPs ($DP^R(i,t)$) and individual large loads ($IL^R(b,t)$) at each hour are defined as the additional load demand reduction of each load for each scenario, if compared to its scheduled load demand reduction. Choosing the maximum value guarantees that the scheduled load reserve can cover load reduction's requirement in all scenarios.

$$DP^{R}(i,t) \geqslant DP^{s}(i,t,s)-DP^{E}(i,t) \quad \forall s,i,t \tag{27}$$

$$IL^{R}(b,t) \geqslant IL^{s}(b,t,s)-IL^{E}(b,t) \quad \forall s,b,t \tag{28}$$

The reactive power reduction of each load in the demand response program is considered proportional to the active power reduction according to the power factor of the considered load.

4.2.3. DG power and reserve constraints

The DG units have a maximum and minimum generating capacity beyond which it is not feasible to generate due to technical reasons. Generating limits are specified as upper and lower limits for the real and reactive power outputs.

$$P_{DG}(j,t)+R_{DG}(j,t) \leqslant P_{DGj}^{max}\cdot u(j,t) \quad \forall j,t \tag{29}$$

$$P_{DG}(j,t) \geqslant P_{DGj}^{min}\cdot u(j,t) \quad \forall j,t \tag{30}$$

where P_{DGj}^{min} and P_{DGj}^{max} are the minimum and maximum limits of j th DG output power, respectively; $u(j,t)$ represents the on/off state of jth DG.

The start up cost ($SU(j,t)$) of the DG units is calculated as follows:

$$SU(j,t)=Scost(j)\times(u(j,t)-u(j,t-1)) \tag{31}$$

$$SU(j,t) \geqslant 0 \tag{32}$$

where $Scost(i)$ is the start up cost of jth DG.

The spinning reserves ($R_{DG}(j,t)$) provided by DGs and the main grid ($R_{grid}(t)$) are calculated as follows:

$$R_{DG}(j,t) \geqslant Ps_{DG}(j,t,s)-P_{DG}(j,t) \quad \forall j,t,s \tag{33}$$

$$R_{grid}(t) \geqslant Ps_{grid}(s,t)-P_{grid}(t) \quad \forall s,t \tag{34}$$

The ramp-rate limits of DGs are given as follows [38]:

$$P_{DG}(j,t)-P_{DG}(j,t-1) \leqslant RU_{j} \quad \forall j,t \tag{35}$$

$$P_{DG}(j,t-1)-P_{DG}(j,t) \leqslant RD_{j} \quad \forall j,t \tag{36}$$

where RU_j and RD_j represent, respectively, ramp-up and ramp-down rate limits of DG j

The minimum up/down time limits of DGs are given as follows [38]:

$$\left[X_{j}^{on}(t-1)-T_{j}^{on}\right]\times[u(j,t-1)-u(j,t)] \geqslant 0 \quad \forall j,t \tag{37}$$

$$\left[X_{j}^{off}(t-1)-T_{j}^{off}\right]\times[u(j,t)-u(j,t-1)] \geqslant 0 \quad \forall j,t \tag{38}$$

where $X_j^{on}(t)$ and $X_j^{off}(t)$ represent, respectively, the time duration for which DG j has been on and off in period t; T_j^{on} and T_j^{off} are the minimum up and down time of DG j, respectively.

4.2.4. Power flow constraints

$$P_{inj}(n,t)=\sum_{m=1}^{N}|V(n,t)||V(m,t)||Y_{n,m}|\cos(\delta(m,t)-\delta(n,t)+\theta_{n,m}) \quad \forall n,t \tag{39}$$

$$Q_{inj}(n,t)=-\sum_{m=1}^{N}|V(n,t)||V(m,t)||Y_{n,m}|\sin(\delta(m,t)-\delta(n,t)+\theta_{n,m}) \quad \forall n,t \tag{40}$$

where N is the total number of buses; n and m are indexes for buses; $|V(n,t)|$ is the voltage amplitude at node n; $\delta(n,t)$ is the voltage angle at node n; $|Y_{n,m}|$ is the element (n,m) of the admittance matrix; $\theta_{n,m}$ is the angle of $Y_{n,m}$; $P_{inj}(n,t)$ and $Q_{inj}(n,t)$ are the net injected active and reactive power to node n, respectively.

The other network operation constraints are as follows:

$$|S(n,m,t)| \leqslant S_{n,m}^{max} \quad \forall n,m,t \tag{41}$$

$$V_{n}^{min} \leqslant V(n,t) \leqslant V_{n}^{max} \quad \forall n,t \tag{42}$$

$$P_{sub}(t) \leqslant P_{sub}^{max} \quad \forall t \tag{43}$$

where $|S(n,m,t)|$ is the apparent power flow from node n to m; $S_{n,m}^{max}$ is the capacity of the line/cable between node n and node m; V_n^{max} and V_n^{min} are the maximum and minimum voltage magnitudes at node n, respectively; $P_{sub}(t)$ is the power output from the main substation.

4.3. Multi-objective mathematical programming problems

In Multiobjective Mathematical Programming (MMP) there are different objective functions and there is no single optimal solution that simultaneously optimizes all the objective functions. In MMP the concept of optimality is replaced with that of efficiency or Pareto optimality. The efficient (or Pareto optimal, non-dominated, non-inferior) solutions are the solutions that cannot be improved in one objective function without deteriorating their performance in at least one of the rest [39]. In these cases the decision makers are looking for the "most preferred" solution. The method that has been used in this paper is augmented ε-constraint method.

This method is described as follows and more details are available in [40,41].

4.3.1. Augmented ε-constraint method

In the proposed method, there is a challenge between reducing the cost and the amount of air pollutants emissions produced by conventional generators. In order to assess the trade-off between reducing the cost and the amount of air pollutants emissions produced by conventional generators, augmented ε-constraint method is used in the proposed method.

For this model, only the range of the objective function $F^{Emission}$ is calculated in the augmented ε-constraint method, while F^{cost} is the main objective function. Then, the range of the objective function $F^{Emission}$ is divided to k equal intervals. Therefore, there are in total $(k+1)$ grid points for $F^{Emission}$. Thus, $(k+1)$ optimization subproblems must be solved where some of these subproblems may have infeasible solution space. The problem has the following form [40,41]:

$$\min\left(F^{cost} - \delta \times \left(\frac{S_2}{r_2}\right)\right) \tag{44}$$

subject to:

$$F^{Emission} + S_2 = \varepsilon_2,\ S_2 \in R^+$$

where

$$\varepsilon_2 = F^{Emission}_{max} - \left(\frac{F^{Emission}_{max} - F^{Emission}_{min}}{q_2}\right) \times k, \quad k = 0, 1, \ldots, q_2 \tag{45}$$

where δ is a small number (usually between 10^{-3} and 10^{-6}); S_2 is an interval variable; $F^{Emission}_{max}$ and $F^{Emission}_{min}$ represent the maximum and minimum values of the individual objective function, total air pollutants emission, based on the payoff table, respectively; ε_2 is the kth range of $F^{Emission}$; r_2 is the range of the total air pollutants emission $\left(F^{Emission}_{max} - F^{Emission}_{min}\right)$, and q_2 is the number of equal part.

When solving each of the sub problems all the constraints of the model should be also considered. By solving each optimization sub-problem, one Pareto-optimal solution is obtained. With higher number of grid points, a denser efficient set is obtained but with a higher computational time. A trade-off between the density of the efficient set and time consuming is always necessary. In this paper, the number of intervals for the objective function $F^{Emission}$ is considered to be equal to 10.

4.3.2. Best compromise solution

When the Pareto-optimal solution is obtained, one of the solutions is chosen as the best compromise solution. Fuzzy sets are introduced here to handle the problem [42] and a linear membership function (μ_i^k) is described for each of the objective functions, i.e. F^{Cost} and $F^{Emission}$:

$$\mu^k_{i\ i=cost,emission} = \begin{cases} 1, & F_i^k \leqslant F_i^{min} \\ \left[\frac{F_i^{max} - F_i^k}{F_i^{max} - F_i^{min}}\right], & F_i^{min} \leqslant F_i^k \leqslant F_i^{max}, \\ 0, & F_i^k \geqslant F_i^{max} \end{cases} \tag{46}$$

where F_i^k and μ_i^k represent the value of the ith objective function in the kth Pareto-optimal solution and its membership function, respectively. For each of the k solutions, the membership function can be normalized as follows:

$$\mu^k = \frac{\sum_{i=1}^{p}\omega_i\mu_i^k}{\sum_{k=1}^{m}\sum_{i=1}^{p}\omega_i\mu_i^k} \tag{47}$$

where ω_i is the weight value of the ith objective function in the MMP problem also, m is the number of Pareto-optimal solutions. The weight values ω_i can be selected by the operator based on the importance of economic issue and environmental allowance. The solution with the maximum membership function μ^k is the most preferred compromise solution based on the implemented weight factors and so is selected as the best Pareto-optimal solution.

4.4. Computation technique

The energy and reserve scheduling problem formulated in the paper is a large-scale Mixed Integer Nonlinear programming (MINLP) optimization problem. MINLP optimization techniques require significant computer means and the execution times are not compatible with the short-term energy and reserve scheduling [14,16]. Therefore, it is necessary to use alternative methodologies in order to have fast response for optimization problems with many variables. In order to make the proposed model applicable for real size distribution networks with large number of consumers and overcome the difficulties related to the solution of nonlinear optimization problems with binary variables, a fast and robust optimization technique, known as Benders decomposition, is implemented in this paper [43]. The use of Benders decomposition to address optimization problems allows a lower processing time if compared with MINLP approaches for solving large dimension complex problems. The proposed solution technique is also designed for real size smart distribution systems scheduling in which there are time-coupling constraints like ramping constraints and minimum operation time, as well as energy storages and electric vehicles. The distribution energy resource scheduling is known as a complex MINLP optimization problem and the proposed solution method could significantly reduce the execution time of the day-ahead energy and reserve scheduling.

The basic idea behind this method is to decompose the problem into two simpler parts: the first part, called master problem, solves a relaxed version of the problem and get values for a subset of the variables. The second part, called sub-problem (or auxiliary problem), receives the values for the remaining variables, while keeping the first ones fixed, and uses these to generate cuts for the master problem [44]. The master and auxiliary problems are solved iteratively until no more cuts can be generated. The combination of the variables found in the last master and sub-problem iteration is the solution to the original formulation. This method allows appropriately treating the non-convexity associated with binary variables and dividing the global problem into two smaller problems which are easier to solve.

As shown in Fig. 7, the master problem consists of 24-h multiobjective energy and reserve scheduling problems which are solved by using the mixed-integer linear programming (MILP) solver CPLEX [45]. The sub-problem is an hourly distribution power flow, with some fixed variables received from the master problem solution, and is solved using non-linear programming (NLP) solver CONOPT [46]. Both the master and the sub-problem are modeled in GAMS [47] on a Pentium IV, 2.6 GHz processor with 4 GB of RAM. More details on Benders decomposition and its features are available in [48] and its implementation in optimal power flow problems is described in [10].

The master problem's objective function is formulated as:

$$Min\, F^{cost} + \sum_{t=1}^{T}\alpha_t^* \tag{48}$$

Subject to constraints (25)–(38) as well as to emission constraint calculated by the augmented epsilon constraint method. The Benders cut is calculated as follows:

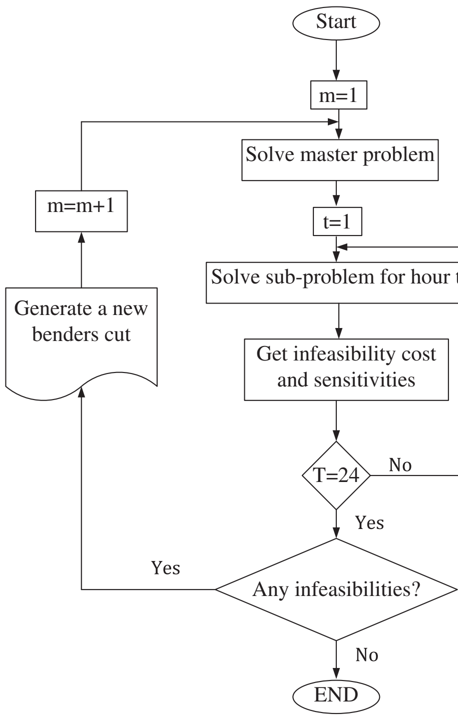

Fig. 7. Benders decomposition flowchart.

$$\alpha_t^* \geqslant \alpha_t^{m-1} + \lambda_{sub,t}^{m-1} \times \left(P_{grid}(t) - \overline{P_{grid}}(t)^{m-1}\right) + \sum_{j=1}^{J} \mu_{j,t}^{m-1} \times \left(P_{DG}(j,t) - \overline{P_{DG}}(j,t)^{m-1}\right) \quad (49)$$

where α_t^* is the sub-problem cost at iteration $m-1$. The Benders linear cuts (49) couple master and sub-problem, and are updated at each iteration.

The sub-problem checks the feasibility of the master problem solution by mean of an AC power flow. Then, any violations in constraints (41)–(43) can be relieved by adjusting the imported power through substation and output power of DGs. The objective function introduced in (50) minimizes the cost of deviations from the master problem solution:

$$Min \sum_{t=1}^{T} \left[\sum_{n=1}^{N} \widetilde{P}_{sv}(n,t) + \widetilde{Q}_{sv}(n,t) \right] \quad (50)$$

where $\widetilde{P}_{sv}(n,t)$, $\widetilde{Q}_{sv}(n,t)$ represent, respectively, the requirements of real power, reactive power at node n and in period t. In other words, they are the slack variables of the optimization problem that are necessary to make the optimization problem feasible.

$$P_{inj}(n,t) + \widetilde{P}_{sv}(n,t) = \sum_{m=1}^{N} |V(n,t)||V(m,t)||Y_{n,m}| \cos(\delta(m,t) - \delta(n,t) + \theta_{n,m}) \quad \forall n,t \quad (51)$$

$$Q_{inj}(n,t) + \widetilde{Q}_{sv}(n,t) = -\sum_{m=1}^{N} |V(n,t)||V(m,t)||Y_{n,m}| \sin(\delta(m,t) - \delta(n,t) + \theta_{n,m}) \quad \forall n,t \quad (52)$$

$$P_{grid}(t) = \overline{P_{grid}}(t)^{m} \leftrightarrow \lambda_{sub,t}^{m-1} \quad \forall t \quad (53)$$

$$\left(P_{DG}(j,t) = \overline{P_{DG}}(j,t)^{m}\right) \leftrightarrow \mu_{j,t}^{m-1} \quad \forall j,t \quad (54)$$

Constraints (53) and (54) provide the marginal data ($\lambda_{sub,t}$ and $\mu_{j,t}$) associated with the decision taken by the master problem, that is, the sensitivity for each value of the decision variables ($P_{grid}(t)$ and $P_{DG}(j,t)$) fixed by the master problem at the same iteration. These sensitivities are going to be applied to the formulation of the Benders cuts of the following iteration.

The Benders decomposition procedure stops when the solution provided by the master problem is feasible, that is, the value of the objective function computed in the slave problem is zero. This approach to Benders decomposition guarantees method convergence for the considered problem.

Even if the Benders decomposition does not guarantee to obtain the global optimum in all types of problems, the Benders technique is able to find the global optimum in some MINLP optimization problems [49–51]. In other cases, the Benders method convergence should be examined. In order to demonstrate that the proposed method allows obtaining the global optimum, the results obtained with the Benders method have been compared with those obtained by using a robust MINLP commercial solver. In particular, in order to validate the proposed method, the hourly scheduling problem with a MINLP commercial solver in GAMS was examined. The results of these two methods have been compared and equal results have been obtained from the benders decomposition method. The comparison confirmed that the proposed computation technique is able to find the optimal solution.

5. Case study

The proposed method was applied to a modified version of the 41-bus 11.4-kV radial distribution system given in [52] and illustrated in Fig 8. The main substation at bus 1 is used to feed rural area with a peak load of 16.8 MW.

Table 1 provides the hourly energy price of Ontario electricity market on Wednesday 23 January 2013 [53]. The capacity cost for spinning reserve from the main grid is, instead considered to be equal to the 25% of the hourly energy price at each hour. The forecasted load profile of the test system for a 24-h period is shown in Fig. 9. Real average hourly wind speed is shown in Fig. 10 [54]. All wind turbines installed in the test system are of the same type with specifications power rated of 1.1 MW, cut-in speed of 4 m/s, nominal speed of 14 m/s, and cut-out speed of 25 m/s. The wind turbines are located at buses 15, 19, 26, 29, 32, 35, 41. Also, two diesel generator sets are installed at buses 14 and 28. Wind turbines and diesel generators are assumed to have fixed power factors of 1 and 0.9 lagging, respectively. The VOLL, required to estimate the social cost of interruptions, is assumed to be 1000 $/MW h [55].

The Load buses areas of each DRP are shown in Table 2. The DRPs' price–quantity offer package, which is in the format of the package presented in Section 2, is presented in Fig. 11. It is assumed that individual loads (IL) participating in the DR program are located at buses 7, 40 and 31 and their offer packages are given in Table 3.

The fuel cost and emission rate of the two diesel generator units are given in Table 4 [9,56,57]. The minimum up and down time of the diesel generators are assumed to be one hour. The spinning reserve of DGs is priced at a rate equal to the 25% of their highest marginal cost of the energy production [58]. The main grid generation system is typically composed of nuclear, hydro, gas steam, coal and gas combined cycle power plants. In this case study, it is supposed, therefore, that, according to a unit commitment program at each hour, the average CO_2 emission rates of conventional power plants in the main grid for low (hours 23–24 and 1–6), medium (hours 6–20) and high (hours 20–23) load hours are of 200, 562, 985 kg/MWh, respectively [57].

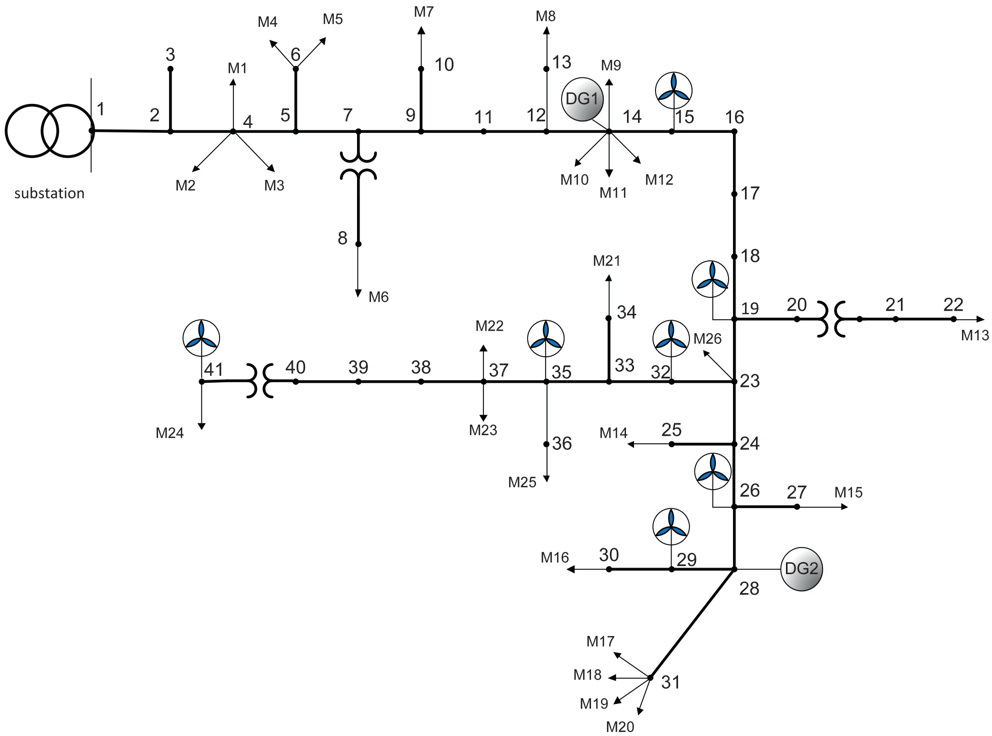

Fig. 8. Forty-one bus distribution test system.

Table 1
Hourly price of the open market.

Hour	Price ($/MW h)	Hour	Price ($/MW h)
1	47.47	13	60.64
2	31.64	14	40.88
3	31.65	15	28.50
4	32.60	16	38.75
5	40.78	17	35.55
6	38.64	18	112.42
7	158.95	19	575.58
8	384.14	20	87.72
9	67.27	21	35.06
10	52.29	22	47.18
11	44.59	23	61.27
12	108.49	24	33.90

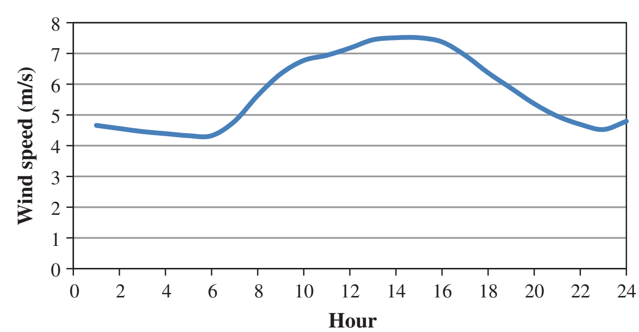

Fig. 10. Hourly wind speed forecast.

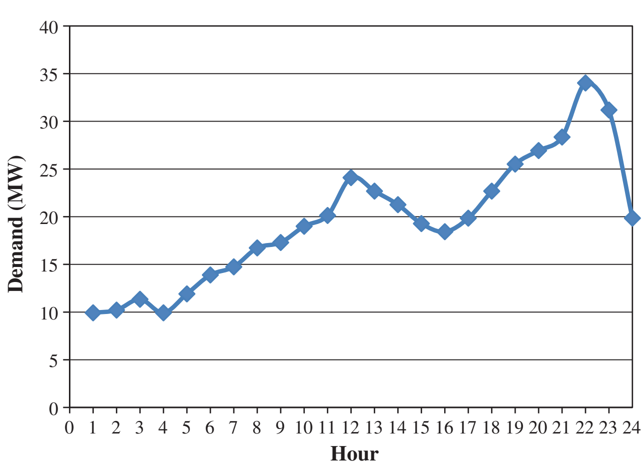

Fig. 9. Forecasted load profile of the distribution test system.

Table 2
DRPs' support area.

DRP	Bus
DRP1	4, 5, 6
DRP2	10, 13, 14
DRP3	34, 36, 37
DRP4	25, 27, 30

In order to analyze the effects of demand side participation in energy and reserve scheduling as well as of the emission reduction target, the proposed method is tested in three different cases:

- *Case 1:* considering only the cost objective function without a DR program;
- *Case 2:* considering only the cost objective function with a DR program;
- *Case 3:* considering the multi-objective optimization.

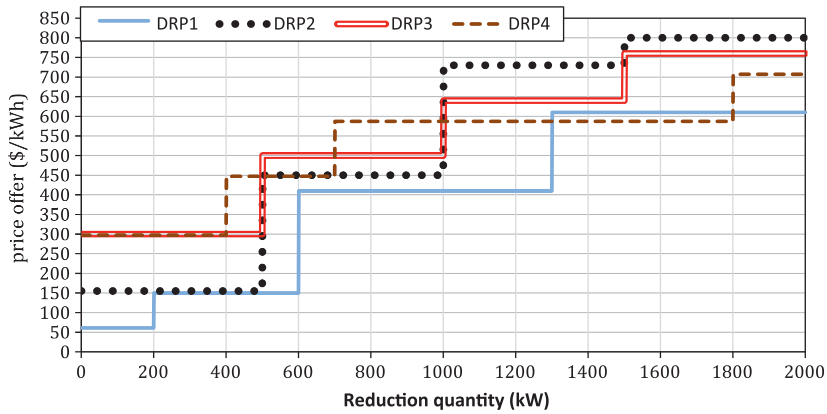

Fig. 11. Price–quantity offer package of DRPs.

Table 3
Individual load offer.

IL number	Bus	Quantity (kW)	Price ($/kW h)
1	13	400	321
2	29	1400	126
3	72	350	418
4	76	1000	580
5	80	1200	145

Table 4
Emission rate of generation sources.

Unit	Cost coefficient				Technical constraints		Emission
	a_j ($)	b_j ($/MW h)	c_j ($/MW h^2)	Startup ($)	P_{min} (MW)	P_{max} (MW)	CO_2 (kg/MW h)
DG1	48.40	123	153.9	1	0.08	1.1	740
DG2	31	98	120	1.2	0.05	1.2	890

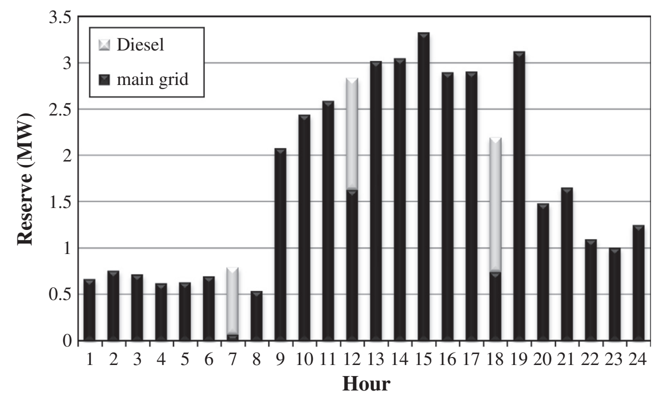

Fig. 12. Scheduled reserve in Case without considering DR.

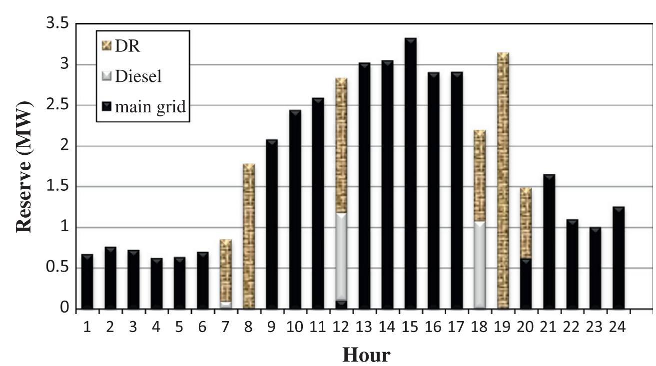

Fig. 13. Scheduled reserve in Case with DR.

5.1. Cost minimization in cases 1 and 2

The results of the optimization problem considering only the cost objective function are given in Table 5. The costs of energy and reserve considering the main grid, diesel generators and demand response, are compared in the two cases with and without demand side participation. As shown in Table 5, simulation results evidence that the proposed method allows obtaining lower total operation costs when considering DR programs.

The scheduled reserve in these two cases is shown in Figs. 12 and 13. Its worth nothing that, due to the reserve prices, when considering the case with DR participation, the scheduled reserve from the main grid is reduced during hours 8, 12, 18, 19 and 20. Moreover, the DR participation in reserve scheduling allows releasing the diesel generator capacity for delivering energy during hour 7.

5.2. Multi-objective optimization

In this case, the energy and reserve scheduling is carried out considering both cost and emissions as objective functions. The Augmented ε-constraint method is implemented in order to carry out the multi-objective optimization. The results from the individual optimization of the cost and emission functions are shown in Table 6 (payoff table). From the payoff table, the range of the emission objective function is obtained and used as constraint in augmented ε-constraint method.

Table 5
Scheduling cost comparison in two cases: with and without DR.

Cost ($)	Wind power	Main grid		Diesel generator		DR		Total	
		Energy	Reserve	Energy	Reserve	Energy reduction	Reserve	Cost ($)	Emission (Ton)
Without DR	3008	18,991	592	1005	63	–	–	23,659	122.85
With DR	3008	15,441	429	1047	41	2175	75	22,216	118.30

Table 6
Payoff table of the augmented ε-constraint method.

Function	Cost minimization	Emission minimization
Cost (k$)	36.763	118.301
Emission (Ton)	242.209	29.054

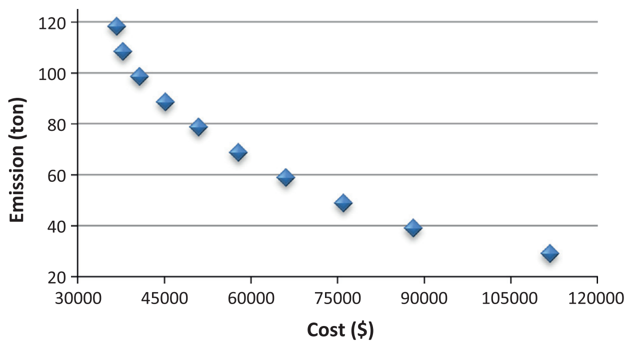

Fig. 14. Pareto-optimal front of the multi-objective method.

Table 7
Fuzzy based procedure used to determine the best compromise solution.

Pareto points (k)	Cost ($)	Emission (ton)	μ_1^k	μ_2^k	μ^k
1	36,763	118.3	1.000	0.000	0.087
2	37,776	108.38	0.995	0.111	0.092
3	40,683	98.47	0.981	0.222	0.096
4	45,178	88.55	0.959	0.333	0.099
5	50,930	78.64	0.931	0.444	0.102
6	57,825	68.72	0.897	0.556	0.104
7	66,012	58.8	0.858	0.667	0.106
8	75,993	48.88	0.809	0.778	0.107
9	88,063	38.97	0.750	0.635	0.106
10	111,746	29.05	0.635	1.000	0.102
The best compromise solution	75,993	48.88	0.809	0.778	0.107

The Pareto-optimal set, obtained from the augmented ε-constraint, is shown in Fig. 14. The membership functions are used to evaluate each member of the Pareto-optimal set. Then the best compromise solution, having the maximum value of the membership function, can be obtained. It should be mentioned that it has been assumed $w_1 = w_2 = 0.5$ as the same importance for the two objectives in the multi-objective problem is considered. Table 7 represents the above procedure in a tabular form.

In order to evaluate the effect of the inclusion of the objective function related to emissions reduction in the proposed model, the best compromise solution derived from the multi-objective method is compared with the solution related to the case 2, in which a single objective function, related to the operational cost, has been considered. Figs. 15 and 16 show the scheduled energy in cases 2 and 3, respectively.

As shown in Fig. 15, the power generation from diesel generators and the load curtailment have been contracted at hours 7, 8, 12, 18 and 19 when the electricity price is higher, thus allowing a reduction of the operational costs. When considering also the objective related the air pollutant reduction, the scheduling results change. As shown in Fig. 16, the load curtailment has been contracted during medium and peak hours when the average emissions rate of the main grid power plants is higher. Moreover, the diesel generators have been committed during hours 19–22 when the emissions rate of the main grid power plant is higher than the emissions rate of the diesel generators. Consequently, in case 3 the emissions related to the energy consumption are reduced if compared to those obtained in case 2.

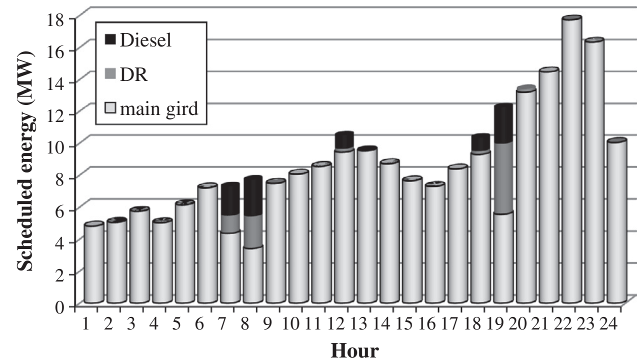

Fig. 15. Scheduled energy in case 2.

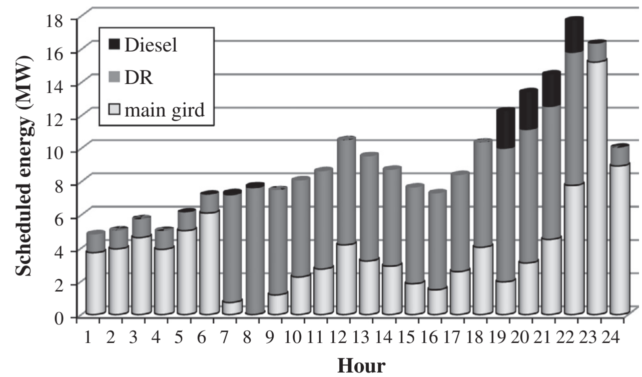

Fig. 16. Scheduled energy in case 3.

Table 8
Best compromise solution with and without DR.

	Energy cost (k$)				Emission (ton)		
	Main grid	Diesel generator	DR	Total	Main grid	Diesel generator	Total
Without DR	20.29	1.02	–	21.31	6.14	115.18	121.32
With DR	10.54	0.89	7.67	19.10	5.052	92.43	97.482

To evaluate the effect of demand side participation in the proposed multiobjective method, the case 3 has also been carried out without considering a DR program. The results related to energy and demand response costs, as well as emissions in the best compromise solutions are shown in Table 8. DR participation has reduced the operational costs due to energy reduction during hours with high electricity prices. Moreover, the DR participation allows reducing the scheduled power from diesel generators, as well as the power imported from the main grid, especially in periods with high emission rates. Consequently, emissions have been reduced due to the DR program.

In order to evaluate the robustness of Benders decomposition method, the proposed model is also solved using a MINLP optimization solver. The case 3 has been solved on a PC, 2.6 MHz with 4 GB of RAM under GAMS software [47]. For MINLP optimization, DICOPT solver [59] has been used. The cost objective values and execution times obtained with the two methodologies for

Table 9
Comparison between the execution time required to obtain the optimal solution.

Method	Cost objective ($)	Execution time (s)
Benders decomposition	75,993	12
MINLP	75,993	1856

executing only the best compromised case is shown in Table 9. In this test case the Benders decomposition method achieved a lower execution time.

6. Conclusion

In this paper, an energy and reserve scheduling method for distribution systems with demand side participation has been proposed. A two stage stochastic approach was used to integrate the probabilistic nature of wind generation and demand into a multi-objective energy and reserve scheduling program. The generalized Benders decomposition method was used in order to solve the proposed large-scale multi-period problem. The method evidences good convergence properties and the simulation results demonstrate that the demand participation in energy and reserve scheduling allows reducing the total operation costs. In order to show the capability of the multi-objective optimization, the scheduling has been compared for the single objective and the multi-objective problems. Simulation results evidenced that the inclusion of the emission objective function determines a variation of the scheduling results in order to reduce the total air pollutant emission. Moreover, the Benders decomposition method permits a significant reduction in the required execution time and allows, therefore, applying the proposed model to real size distribution systems, or to the future smart grid consisting of huge amount of distributed resources.

References

[1] The promotion of electricity produced from renewable energy sources in the internal electricity market. Directive 2001/77/EC of the European Parliament and of the Council; 2001.
[2] Kyoto protocol to the United Nations framework convention on climate change. Accra climate change talks; 2008. <http://unfccc.int/meetings/intersessional/accra/items/4437.php>.
[3] The limitation of emissions of certain pollutants into the air from large combustion plants. Directive 2001/80/EC of the European Parliament and of the Council; 2001, October. <http://www.europa.eu.int>.
[4] National emission ceilings for certain atmospheric pollutants. Directive 2001/81/EC of the European Parliament and of the Council. <http://europa.eu/legislation_summaries/environment/air_pollution/l28095_en.htm>.
[5] Denny E, O'Malley M. Wind generation power system operation and emissions reduction. IEEE Trans Power Syst 2006;21:341–7.
[6] Sauter T, Lobashov M. End-to-end communication architecture for Smart Grids. IEEE Trans Ind Electron 2011;58:1218–28.
[7] Siano P, Cecati C, Yu H, Kolbusz J. Real time operation of smart grids via FCN networks and optimal power flow. IEEE Trans Ind Inform 2012;8:944–52.
[8] Medina J, Muller N, Roytelman I. Demand response and distribution grid operations: opportunities and challenges. IEEE Trans Smart Grid 2010;1:193–8.
[9] Cecati C, Citro C, Siano P. Combined operations of renewable energy systems and responsive demand in a smart grid. IEEE Trans Sust Energy 2011;2:468–76.
[10] Khodr HM, Martínez-Crespo J, Matos MA, Pereira J. Distribution systems reconfiguration based on OPF using Benders decomposition. IEEE Trans Power Del 2009;24:2166–76.
[11] Vahidinasab V, Jadid S. Joint economic and emission dispatch in energy markets: a multiobjective mathematical programming approach. Energy 2010;35:1497–504.
[12] Kuo CC. Generation dispatch under large penetration of wind energy considering emission and economy. Energy Convers Manage 2010;51:89–97.
[13] Harrison GP, Piccolo A, Siano P, Wallace AR. Exploring the trade-offs between incentives for distributed generation developers and DNOs. IEEE Trans Power Syst 2007;22:821–8.
[14] Silva M, Morais H, Vale Z. An integrated approach for distributed energy resource short-term scheduling in smart grids considering realistic power system simulation. Energy Convers Manage 2012;64:273–88.
[15] Broeer T, Fuller J, Tuffner F, Chassin D, Djilali N. Modeling framework and validation of a smart grid and demand response system for wind power integration. Appl Energy 2014;113:199–207.
[16] Soares J, Morais H, Sousa T, Vale Z, Faria P. Day-ahead resource scheduling including demand response for electric vehicles. IEEE Trans Smart Grid 2013;4:596–605.
[17] Assessment of demand response and advanced metering, FERC, staff report, Docket No. AD06-2, August 7, 2006.
[18] NIST framework and roadmap for smart grid interoperability standards, January 2010. <www.nist.gov/smartgrid>.
[19] Boyle G. Renewable energy. Oxford, UK: Oxford Univ. Press; 2004.
[20] Ortega-Vazquez MA, Kirschen DS. Economic impact assessment of load forecast errors considering the cost of interruptions. In: Proc IEEE power eng soc general meeting, Montreal, QC, Canada, 2006. p. 8.
[21] Yan HM, Yan HZ. Optimal energy purchases in deregulated California energy markets. Proc IEEE Power Eng Soc Winter Meeting 2000;2:1249–54.
[22] Ortega-Vazquez M, Kirschen D. Estimating spinning reserve requirements in systems with significant wind power generation penetration. IEEE Trans Power Syst 2009;24:114–24.
[23] Makarov Y, Loutan C, Ma J, de Mello P. Operational impacts of wind generation on California power systems. IEEE Trans Power Syst 2009;24:1039–50.
[24] Doherty R, O'Malley M. A new approach to quantify reserve demand in systems with significant installed wind capacity. IEEE Trans Power Syst 2005;20:587–95.
[25] Bouffard F, Galiana FD. Stochastic security for operations planning with significant wind power generation. IEEE Trans Power Syst 2008;23:306–16.
[26] Hoyland K, Wallace SW. Generating scenario trees for multistage problems. Manage Sci 2001;47:295–307.
[27] Gulpinar N, Rustem B, Settergren R. Simulation and optimization approaches to scenario tree generation. J Econ Dynam Control 2004;28:1291–315.
[28] EURELECTRIC. The role of distribution system operators (DSOs) as information hubs – A EURELECTRIC networks committee paper; 2010. <http://www.eurelectric.org/media/44143/role_of_dsos_as_information_hubs_final_draft_10-06-10-2010-200-0001-01-e.pdf>.
[29] EU. More Microgrids – Advanced architectures and control concepts for more microgrids-European Research Project, December 2009.
[30] Bouffard F, Galiana FD, Conejo AJ. Market-clearing with stochastic security––Part I: Formulation. IEEE Trans Power Syst 2005;20:1818–26.
[31] Caltech Resnick Institute. Grid 2020 towards a policy of renewable and distributed energy resources. Resnick Institute Report, September 2012. <http://resnick.caltech.edu/learn/docs/GRID_2020_Resnick%20Report.pdf>.
[32] Birge JR, Louveaux F. Introduction to stochastic programming. New York: Springer-Verlag; 1997.
[33] Mokryani G, Siano P. Evaluating the integration of wind power into distribution networks by using Monte Carlo simulation. Int J Electric Power 2013;53:244–55.
[34] Siano P, Mokryani G. Probabilistic Assessment of the impact of wind energy integration into distribution networks. IEEE Trans Power Syst 2013;28:4209–17.
[35] Siano P, Mokryani G. Assessing wind turbines placement in a distribution market environment by using particle swarm optimization. IEEE Trans Power Syst 2013;28:3852–64.
[36] Wood AJ, Wollenberg FB. Power generation, operation and control, book. New York: John Wiley & Sons, Ltd.; 1996.
[37] Wang J, Redondo NE, Galiana FD. Demand-side reserve offers in joint energy/reserve electricity markets. IEEE Trans Power Syst 2003;18:1300–6.
[38] Wang C, Shahidehpour SM. Effects of ramp-rate limits on unit commitment and economic dispatch. IEEE Trans Power Syst 1993;8:1341–50.
[39] Collette Y, Siarry P. Multiobjective optimization: principles and case studies. Berlin: Springer; 2003.
[40] Mavrotas G. Generation of efficient solutions in multiobjective mathematical programming problems using GAMS. <http://www.gams.com>.
[41] Mavrotas G. Effective implementation of the ε-constraint method in multi-objective mathematical programming problems. Appl Math Comput 2009;213:455–65.
[42] Agrawal S, Panigrahi BK, Tiwari MK. Multiobjecive particle swarm algorithm with fuzzy clustering for electrical power dispatch. IEEE Trans Evolut Comput 2008;12:529–41.
[43] Benders JF. Partitioning procedures for solving mixed-variables programming problems. Numer Math 1962;4:238–52.
[44] Geoffrion AM. Generalized Benders decomposition. J Optim Theor Appl 1972;10:237–60.
[45] CPLEX manual – GAMS. <www.gams.com/dd/docs/solvers/cplex.pdf>.
[46] CONOPT manual – GAMS. <http://www.gams.com/dd/docs/solvers/conopt.pdf>.
[47] Brooke A, Kendrick D, Meeraus A, Raman R. GAMS: a user's guide. Washington, DC: GAMS Development Corporation; 1998.
[48] Shahidehpour M, Fu Y. Tutorial: benders decomposition in restructure power systems. <http://motor.ece.iit.edu/ms/benders.pdf>.
[49] Geoffrion AM. Generalized Benders decomposition. J Optimiz Theor Appl 1972;10:237–60.
[50] Floudas CA, Aggarwal A, Ciric AR. Global optimum search for nonconvex NLP and MINLP problems. Comput Chem Eng 1989;13:1117–32.
[51] Sahinidis V, Grossmann IE. Convergence properties of generalized Benders decompositions. Technical report; 1990. <http://repository.cmu.edu/cheme/171/>.

[52] Atwa YM, El-Saadany EF. Probabilistic approach for optimal allocation of wind based distributed generation in distribution systems. IET Renew Power Gener 2011;5:79–88.
[53] Hourly Ontario Energy Price. <https://www.ieso.ca/imoweb/marketdata/hoep.asp>.
[54] http://weather.uwaterloo.ca/data.html.
[55] Bouhouras AS, Labridis DP, Bakirtzis AG. Cost/worth assessment of reliability improvement in distribution networks by means of artificial intelligence. Int J Electric Power Energy Syst 2010;32:530–8.
[56] Strachan ND, Farrell AE. Emissions from distributed generation. CEIC working paper, 2002, 02-04. <http://wpweb2.tepper.cmu.edu/ceic/pdfs/CEIC_02_04.pdf>.
[57] Hadley SW, Van Dyke JW. Emission benefit of distributed generation in the Texas market, U.S. Department of Energy (DOE), April 2003.
[58] Bouffard F, Galiana FD, Conejo AJ. Market-clearing with stochastic security – Part II: Case studies. IEEE Trans Power Syst 2005;20:1827–18353.
[59] DICOPT manual – GAMS. <www.gams.com/dd/docs/solvers/dicopt.pdf>.